Does the Optimum Hydrophilic Lipophilic Balance Condition Affect the Physical Properties of Mixed Reverse Micelles? A Spectroscopic Investigation

ARTICLE *in* THE JOURNAL OF PHYSICAL CHEMISTRY B · MAY 2014

Impact Factor: 3.3 · DOI: 10.1021/jp5028178 · Source: PubMed

2 AUTHORS, INCLUDING:

Arindam Das
S.N. Bose National Centre for Basic Sciences
4 PUBLICATIONS **16** CITATIONS

THE JOURNAL OF PHYSICAL CHEMISTRY B

Article

pubs.acs.org/JPCB

Do the Physical Properties of Water in Mixed Reverse Micelles Follow a Synergistic Effect: A Spectroscopic Investigation

Arindam Das, Animesh Patra, and Rajib Kumar Mitra*

Unit for Nano Science & Technology, Department of Chemical Biological and Macromolecular Sciences, S.N. Bose National Centre for Basic Sciences, Block JD, Sector III, Salt Lake, Kolkata 700098, India

Supporting Information

ABSTRACT: In this contribution we have tried to investigate whether the mechanical properties of the reverse micellar (RM) interface dictate the physical properties of entrapped water molecules in the RM waterpool. We choose AOT/Igepal-520/cyclohexane (Cy) mixed RM as a model system which exhibits synergistic water solubilization behavior as a function of interfacial stoichiometry. Such a phenomenon associates systematic modification of the interface curvature. Dynamic light scattering (DLS) studies reveal linear increase in the droplet size and aggregation number of the RMs with increasing X_{Igepal} (mole fraction of Igepal in the surfactant mixture). FTIR study in the 3000−3800 cm^{-1} region identifies that the relative population of the surface-bound water molecules is higher in AOT RM compared to that in Igepal RM, and in mixed systems it also follows a linear trend with X_{Igepal}. Water relaxation dynamics as probed by time-resolved fluorescence spectroscopy using Coumarin-500 also reveals an overall linear trend with no characteristic feature around the solubilization inflation point. Our study clearly identifies that the physical properties of water in RM are mostly governed by the interfacial stoichiometry and water content, and merely bares any dependence on the mechanical properties of the interface.

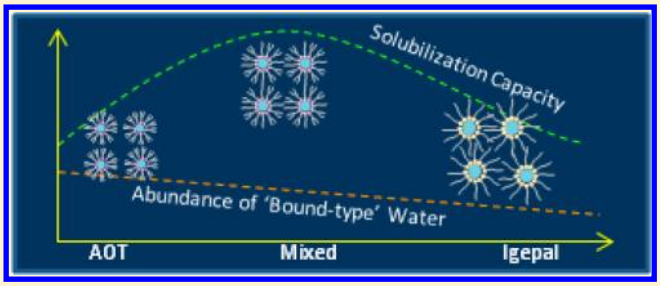

INTRODUCTION

Aggregates of surfactants in oil continuum exhibit the remarkable ability to solubilize a large amount of water to form reverse micelles (RM), which offers a unique platform to realize several constrained environments like living cells.[1] The physical and chemical properties of water molecules localized in the interior of the RMs are different from those of pure water, the difference becoming progressively smaller as the water content in the micellar system increases. When the RM size is small, the interface strongly interacts with most of the water molecules making them "highly structured". Since hydrogen bond dynamics is a concerted process requiring the rearrangement of the hydrogen bonds of many water molecules, the dynamics become relatively slow. This constraint is partially relaxed at higher hydration and the system approaches pure water-like behavior. Solubilization capacity of RM and physicochemical properties of the entrapped water have been found to be strongly dependent on the chemical nature of the dispersant phase (oil), surfactant, and also the hydration level of the RM (w_0 = [water]/[surfactant]).[2,3] Surfactant mixtures often give rise to enhanced performance over the individual components, and such mixtures could potentially be employed in a wide range of practical applications. It has recently been reported that addition of nonionic surfactant into the interface of ionic surfactants produces significant modification of enzyme activity,[4−6] polymer synthesis,[7] nanoparticle synthesis,[8] and chemical activity[9] in RM. A proper rationale of such modified behavior is strongly demanding especially in many biophysical applications that depend on the extent of electrostatic and hydrophobic interactions of the RM interface with specific moiety or segments of solubilized biological macromolecules.[10−12]

Modification of the interface by blending of surfactants brings about considerable changes in the elastic rigidity of the interfacial film. Earlier studies with RM systems involving more than one surfactant using solubilization,[13−16] conductivity,[15,17] interfacial composition,[18] viscosity,[19] spectroscopic,[20−22] SANS,[23−25] and FTIR and NMR measurements[26,27] identify significant modification of the mechanical properties of the interface and consequently of the water structure in RM systems in comparison to the corresponding single surfactant systems. These findings summarize that the effects of surfactant blending on solubilization and other physical properties are a direct consequence of mixing and physicochemical interactions in interfacial films.

It is well-known that water inside RMs is highly structured and its dynamics is highly restricted.[28,29] A recent study[30] has concluded that confinement of water in the RM interior is responsible for the observed slow relaxation dynamics, irrespective of the charge of the interface. On the other hand, Levinger et al.[31−33] compared the ultrafast solvation dynamics of ionic (AOT) and nonionic (Brij-30) RM systems and find

Received: October 17, 2012
Revised: February 11, 2013
Published: March 8, 2013

   dx.doi.org/10.1021/jp3102833 | J. Phys. Chem. B 2013, 117, 3593−3602

that solvation dynamics of the former is slower than that of the latter. A possible source for the observed difference might be the difference in the interaction of water with the charged and uncharged interfaces. However, the effect of mixing of surfactants on the relaxation dynamics of water has only rarely been explored.[34,35]

In a previous study,[36] we attempted to correlate the structure, dynamics, and reactivity of entrapped water in RM consisting of a mixture of ionic (AOT) and non-ionic (Brij-30) surfactant in isooctane, which has a high molecular volume and less penetrability in the surfactant interface. This leads the solubilization capacity of AOT/isooctane RM systems to be limited by the interdroplet interaction effect.[13] AOT/Brij-30 mixed system in isooctane does not offer any synergistic effect in terms of water solubilization capacity. The physical properties of water also showed a linear trend with mixing and it was found that the entrapped water reaches a pure water-like behavior as $X_{Brij\text{-}30}$ (mole fraction of Brij-30 in the surfactant mixture) increases, which is due to the weaker interaction of Brij-30 headgroup with water compared to that of the charged headgroup of AOT. To complement this study, we study the structure and dynamics of a mixed system in which synergistic modification of the surfactant monolayer in terms of solubilization capacity could be realized. The mixture of ionic surfactant AOT and nonionic surfactant Igepal-520 in cyclohexane (Cy) offers such a platform.[16] Both AOT[37] and Igepal CO-520[38] are well-studied surfactants that can form RM without the addition of any cosurfactant. In the present contribution we have studied the structure and slow (sub-ns) relaxation dynamics of water in RMs constituted of AOT and Igepal CO-520 in Cy at different mixing ratios with the key objective to reveal whether the synergistic geometric modification of the interface affects the physical nature of entrapped water. The micellar sizes at different mixing ratios have been measured by the dynamic light scattering (DLS) technique. The physical properties of the entrapped water have been determined using Fourier transform infrared spectroscopy (FTIR), densimetric measurements, and solubility study. Relaxation dynamics of water inside RM has been probed by time-resolved fluorescence spectroscopy using Coumarin 500 (C500) as the fluorophore. This spectroscopic technique, especially the slow relaxation process, which essentially represents the coupled rotational−translational orientation of water molecules, has recently evolved as a potential tool to understand the interaction of confined water molecules with the interface.[36,39−44] Using a fluorophore that essentially resides at the water−surfactant interface, the extent of modification of water dynamics in response to any change in interfacial morphology could be rationalized by probing such relaxation processes. The choice of the probe is based on the fact that, when excited at 409 nm, only the probe molecules residing at the interface and/or facing the polar core get excited.[40] Thus the spectroscopic information obtained is essentially the responses from the interfacial region only, which is a prerequisite for our study. To understand the geometrical restriction of the probe at the interface, rotational relaxation dynamics of the dye in different RM systems have also been determined. All the measurements have been done at six different mixing ratios of AOT and Igepal with the mole fraction of Igepal in the mixture (X_{Igepal} = [Igepal]/([AOT] + [Igepal])), varying as 0, 0.2, 0.4, 0.6, 0.8, and 1 at three hydration levels, namely, w_0 = 5, 10, and 15.

MATERIALS AND METHODS

Sodium bis(2-ethylhexyl) sulfosuccinate (AOT), polyoxyethylene (5) nonylphenyl ether (Igepal-520), cyclohexane (Cy), and Coumarin-500 (C-500) (Scheme 1) were products

Scheme 1. Molecular Structure of AOT, Igepal, and Coumarin 500

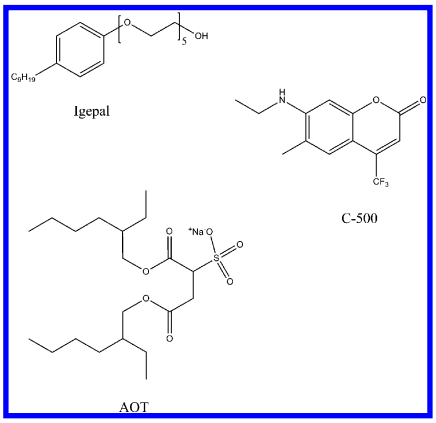

of Sigma-Aldrich. All the chemicals were used without further purification. AOT and Igepal were dissolved in Cy at a concentration of 0.1 (M) to prepare two stock solutions and then mixed in desired proportions. The mole fraction of Igepal, X_{Igepal} = [Igepal]/([AOT] + [Igepal]), was varied from 0 to 1. Calculated amount of water was injected into it to produce the reverse micelles (RMs) of w_0 = 5, 10, and 15.

Water solubilization capacity of these RM systems was determined by titrating a 3 mL surfactant/oil stock solution with dropwise addition of water followed by vigorous shaking in order to ensure the attainment of complete equilibrium. Appearance of persistent visual turbidity and/or phase separation was considered to be the solubilization limit. Average of three successive measurements was taken as the final result.

DLS measurements were carried out with Nano-S Malvern instrument employing a 4 mW He−Ne laser (λ = 632.8 nm) equipped with a thermostatted sample chamber. The details of DLS measurement could be found in our earlier study.[40]

FTIR spectra in the 3000−3800 cm^{-1} window were recorded on a JASCO FTIR-6300 spectrometer (transmission mode) using CaF_2 window. It is important to note that Cy has negligible absorbance in this studied frequency range (data not shown). We herein report difference absorbance spectra, which are the differences between the measured absorbance of the samples and that of the stock solution (at w_0 = 0). For the sample with highest water content (w_0 = 15), the added volume of water is only ∼2% compared to the total volume of the stock solution, indicating that the reduced volume fraction of the stock solution in all the investigated RM systems is negligible. Therefore, the difference spectra can be attributed to the water molecules present in the RM systems only.

High precision density and sound velocity were measured by a density meter: model DSA-5000 from Anton Paar (Austria) with an accuracy of 5 × 10^{-6} g cc^{-1} and 0.5 m s^{-1} in density and sound velocity measurements, respectively. Aggregation number of RM systems was calculated considering the formulations developed in ref 45. The details of the calculation could be found in the Supporting Information section.

dx.doi.org/10.1021/jp3102833 | J. Phys. Chem. B 2013, 117, 3593−3602

Adiabatic compressibility (β) of the mixture can be determined by measuring the solution density (ρ) and the sound velocity (u) and applying the Laplace's equation

$$\beta = \frac{1}{\rho u^2} \tag{1}$$

The apparent specific volume of the solute (water) ϕ_v is given by[46]

$$\phi_v = \frac{1}{\rho_0} + \frac{\rho_0 - \rho}{c\rho_0} \tag{2}$$

where c is the concentration of water in the solution, ρ_0 and ρ are the densities of the dry RM ($w_0 = 0$) and wet RM, respectively. The partial apparent adiabatic compressibility (ϕ_k) of water is obtained from the relation[47]

$$\phi_k = \beta_0\left(2\phi_v - 2[u] - \frac{1}{\rho_0}\right) \tag{3}$$

where $[u]$ is the relative specific sound velocity increment given by

$$[u] = \frac{u - u_0}{u_0 c} \tag{4}$$

where u_0 and u are the sound velocities in dry RM and wet RM, respectively.

Steady-state absorption and emission were measured with Shimadzu UV-2450 spectrophotometer and Jobin Yvon Horiba Fluorolog fluorimeter, respectively. All the measurements were carried out at 298 K. Fluorescence transients were measured and fitted by using commercially available spectrophotometer (Life Spec-ps) from Edinburgh Instrument, U.K. (excitation wavelength 409 nm, 80 ps instrument response function (IRF)). The details of the time-resolved measurements can be found elsewhere.[39] The time dependent fluorescence Stokes shifts, as estimated from time-resolved emission spectra (TRES), were used to construct the normalized spectral shift correlation function or the solvent correlation function C(t) defined as

$$C(t) = \frac{\nu(t) - \nu(\infty)}{\nu(0) - \nu(\infty)} \tag{5}$$

where $\nu(0)$, $\nu(t)$, and $\nu(\infty)$ are the emission maximum (in cm^{-1}) at time zero, t, and infinity, respectively. The $\nu(\infty)$ values had been taken to be the emission frequency beyond which an insignificant or no spectral shift was observed. The $C(t)$ function represents the temporal response of the solvent relaxation process, as occurs around the probe following its photo excitation and the associated change in the dipole moment. For anisotropy, $r(t)$ measurements, emission polarization was adjusted to be parallel or perpendicular to that of the excitation and anisotropy is defined as

$$r(t) = \frac{I_{para}(t) - G.\, I_{perp}(t)}{I_{para}(t) + 2.G.\, I_{perp}(t)} \tag{6}$$

where G, the grating factor, was determined following the long-term tail matching technique.[48] All the anisotropies were measured at the emission maxima.

RESULTS AND DISCUSSION

Solubilization Capacity Measurements. Figure 1 depicts the maximum water solubilization capacity of mixed AOT/Igepal/Cy RM systems. Both AOT and Igepal are fairly soluble in Cy and both these systems solubilize water in the $w_{0,max}$ range of 20−25, which is in good agreement with the data reported in the literature.[16] The mixed surfactant systems exhibit a considerable synergism in the water solubilization capacity wherein $w_{0,max}$ (maximum solubilization capacity) initially increases with increasing X_{Igepal} to pass through a maximum at X_{Igepal} = 0.4 beyond which it decreases. Such synergistic solubilization behavior has previously been reported in a few mixed surfactant systems.[14−16,24,25,49] The extent of water solubilization in general can be explained in light of a theoretical model developed by Hou and Shah.[13] Solubilization capacity of water in RM is geometrically related to the radius of curvature of the surfactant film separating the water droplets from the oil continuum. This in turn is thermodynamically related to the stability of the RM. The stability of a RM is primarily decided by the entropic contribution of droplet dispersion, curvature effect, and the interaction between the droplets.[50,51] The radius of curvature and hence water solubilization capacity decreases as the chain length of oil decreases, chain length of cosurfactant increases, or size of the polar headgroup of the surfactant increases.

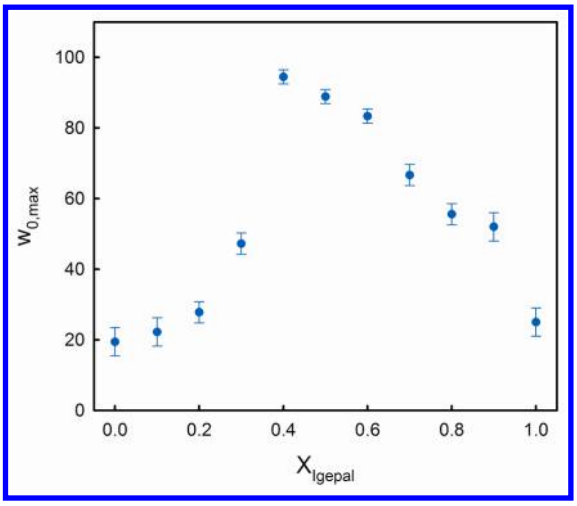

Figure 1. Maximum solubilization capacity ($w_{0,max}$) of AOT/Igepal/Cy mixed reverse micellar systems as a function of X_{Igepal}.

AOT/Cy is a system consisting of a rather rigid interface (owing to the low molecular weight of Cy (~180 Å^3) and high penetration of Cy in the interfacial region making the attractive strength small and favoring greater spontaneous curvature) with very low values of $\Delta\rho$ (difference between densities in the continuous phase and in the penetrable length of the interfacial layer) and ξ (penetrable length of the interfacial layer during interpenetration of droplets). In such a case the interaction among the droplets is very weak compared to the curvature effect, and solubilization capacity is essentially limited by the radius of curvature. Solubilization capacity can be improved if the interface is doped with a second surfactant (herein Igepal 520) which decreases the spontaneous curvature of the interfacial film making the interface more fluid. However, in doing so both $\Delta\rho$ and ξ increase, which in turn increases the interaction between the droplets. The increase in $w_{0,max}$ is

dx.doi.org/10.1021/jp3102833 | J. Phys. Chem. B 2013, 117, 3593−3602

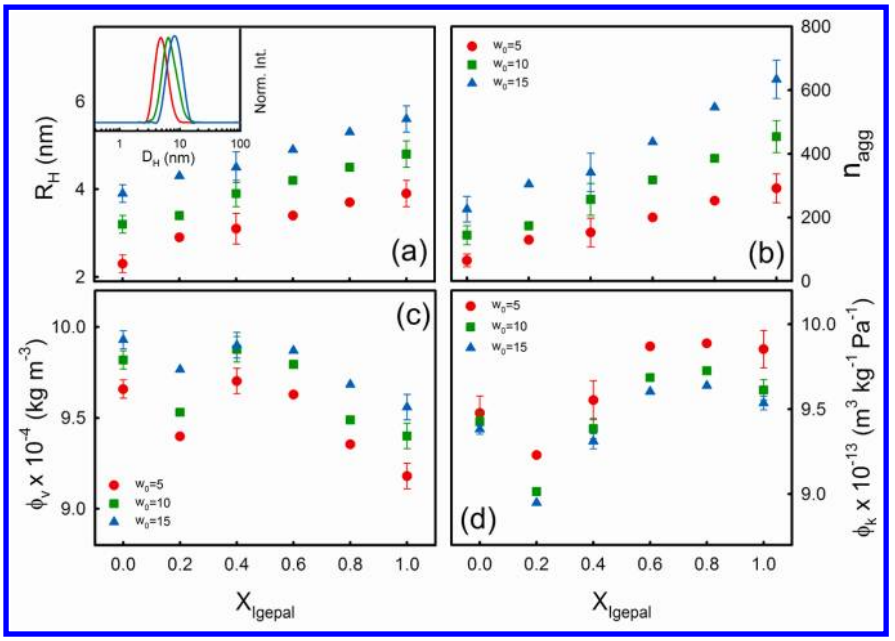

Figure 2. (a) Hydrodynamic radius (R_H) of AOT/Igepal/Cy mixed reverse micellar systems as a function of X_{Igepal}. The inset shows a typical normalized scattering intensity profile of X_{Igepal} = 0 (red), 0.4 (green), and 1.0 (blue) RM systems. (b) The aggregation number (n_{agg}) of the mixed reverse micelles as a function of X_{Igepal}. (c) Specific volume, ϕ_v, and (d) partial apparent adiabatic compressibility, ϕ_k, of water in these mixed reverse micelles at different w_0 values as a function of X_{Igepal}.

limited as the spontaneous radius of curvature approaches the critical radius R_c. Beyond this point the increase in $\Delta\rho$ and ξ decreases $w_{0,max}$. The observed synergism is thus a consequence of systematic alteration of the mechanical properties of the interfacial monolayer which is optimized at X_{Igepal} = 0.4. It is now interesting to investigate whether such a modification imprints the physical properties of the encapsulated water molecules inside the RMs.

DLS, Aggregation Number, and Compressibility Measurements. We measure the size of the RM droplets using DLS technique and the results are depicted in Figure 2a and Table S1 (Supporting Information). The data analysis essentially assumes the droplets to be spherical in nature, and for small w_0 ($\leq$15) values, such an assumption holds well. As observed from the figure, droplet size increases with increase in w_0 as well as X_{Igepal}. The w_0 dependency is a clear consequence of the increasing water load.[40,52] Igepal forms larger droplets compared to AOT[19,38] and this accounts for the increased droplet size of mixed RM systems with increasing X_{Igepal}. No anticipated deviation from linearity in the X_{Igepal} = 0.4 region is unambiguously noticed. This increase in droplet radius with X_{Igepal} is consistent with the hard sphere model of AOT/Cy system as has been discussed earlier. We also measure the droplet size at X_{Igepal} = 0.4 with increasing w_0 values (data not shown). The size increases linearly with w_0 clearly indicating that addition of water increases droplet size rather than forming multiple droplets.

We calculate the aggregation number (n_{agg}) of RM systems and the results are depicted in Figure 2b and Table S1. It is found that Igepal RM systems have higher aggregation number compared to the AOT RM systems. The n_{agg} values obtained for AOT are in good agreement with those reported by Maitra et al. using the NMR technique.[53] It is interesting to note that as Igepal is mixed with AOT n_{agg} increases, which is a consequence of the reduced electrostatic repulsion between the charged head groups of AOT, thereby accommodating more surfactant molecules at the interface. Since surfactant concentration is fixed at 0.1 M, an increase in aggregation number at a fixed w_0 value is indicative of a decrease in the number of water droplets which provides additional support to the increased droplet size as evidenced from DLS measurements (Figure 2a). No considerable change in the aggregation behavior is realized at X_{Igepal} = 0.4. We also calculate the apparent specific volume (ϕ_v) and partial apparent adiabatic compressibility (ϕ_k) of water in these RM systems (Figure 2c,d and Table S1). The obtained ϕ_v values are in the same order of magnitude as obtained for other RM systems[36,54,55] and is smaller than that of pure water (1.003×10^{-3} m^3 kg^{-1}). On the other hand, all the calculated compressibility values are higher than that of pure water (4.5×10^{-10} Pa^{-1}), which essentially indicates the highly structured nature of water inside RM. In all these systems ϕ_v increases with increasing w_0, which is in accordance with previous observations[55] and accounts for the fact that the abundance of high density interfacial water at lower hydration is responsible for the reduced ϕ_v. The ϕ_v values do not exhibit any distinct feature with the mixing ratio; it only reduces marginally as Igepal concentration is increased (Figure 2c). AOT RM systems offer higher ϕ_v values compared to nonionic RM systems[55] which corroborates the present observation of decreasing ϕ_v with increasing nonionic content. The ϕ_k values also exhibit good agreement with previous reports[36,54,55] and offer an overall increasing trend with increasing Igepal concentration. The compressibility data thus provide evidence that water structure is essentially perturbed inside RM due to its interaction with the charged/polar interface; however, the overall linear behavior of the compressibility values indicates that the interfacial stochiometric optimization at X_{Igepal} = 0.4 with regard to water solubilization capacity is not reflected in the physical properties of water.

FTIR Measurements. To obtain a deeper insight into the water structure we measure the MIR FTIR spectra of all the

dx.doi.org/10.1021/jp3102833 | J. Phys. Chem. B 2013, 117, 3593−3602

mixed RM systems. In all these measurements we subtract the data of w_0 = 0 (dry RM) systems from the hydrated systems, and thus the signals essentially provide information from water molecules embodied in the RM water pool. We focus our attention in the 3000−3800 cm^{-1} frequency window as this is a fingerprint region for the symmetric and asymmetric vibrational stretch of O−H bonds in water.[56,57] The overall spectrum of water in this frequency window could be deconvoluted into three Gaussian sub-bands peaking at ∼3600, 3460, and 3330 cm^{-1} regions with relative weightage of ∼5%, 30%, and 65%, respectively (data not shown). The peak at ∼3600 cm^{-1}, i.e., the high frequency component, enjoys the major contributions from the "multimer"[26] water molecules which do not produce strong hydrogen bonds with neighboring water molecules[58] and have generally been realized in extreme hydrophobic environments.[59] The second component peaking at 3460 cm^{-1} involves the so-called "intermediate" water molecules which are unable to form fully developed hydrogen bonds and somewhat connected to other water molecules with distorted H-bonds.[26] Finally, the third kind of water molecule, i.e., the lower frequency component (peaking at 3330 cm^{-1}) emanates from the "network" (sometimes called "bulk type") water molecules which are fully hydrogen bonded with the neighboring water molecules and contributes its majority of share in pure water.

We deconvolute the MIR spectra of all the RM systems into three Gaussian components keeping the peak positions fixed as those of pure water (Figure S1, Supporting Information). A free fitting often produces more accurate contributions; however, fixing the peak positions allows comparison of the change in the relative weightage of each component at variable interfacial compositions. We plot the relative contribution of each curve toward the total spectra and plot it as a function of X_{Igepal} (Figure 3). This relative contribution is proportional to the fraction of water molecules belonging to that particular stretching mode. As evidenced from the figure, the relative abundance of the fully hydrogen bonded water molecules are fewer in RM systems compared to that in pure water; this observation is rather intuitive taking into consideration the interaction of water molecules with both ionic and nonionic RM interfaces.[26,60,61]

The "multimer" water molecules, often identified as the "bound type" water molecules, show characteristic slow dynamics compared to the "network" or "bulk-type" water owing to their strong interaction with the RM interface.[62,63] It can be observed from Figure 3c that the relative abundance of the "multimer" water molecules in AOT RM systems is twice as large as that in pure water. With progressive inclusion of Igepal in the interface, abundance of the "multimer" water decreases. This leads us to conclude that the interaction of water molecules with the polar uncharged headgroup of Igepal is weaker in comparison to that of ionic AOT. With increasing w_{Igepal}, the content of "multimer" water molecules decreases and at high X_{Igepal} it eventually reaches a value comparable to that in pure water. The population corresponding to the "intermediate" water (peaking at 3460 cm^{-1}) shows a marginal variation with both interfacial stoichiometry as well as water content. However, an overall weak decreasing trend is observed with increasing X_{Igepal}.

Let us now consider the population of "network" water (peaking at 3330 cm^{-1}); it is observed that in AOT RM systems the population of such type of water molecules is considerably lower than that in pure water (Figure 3a). This

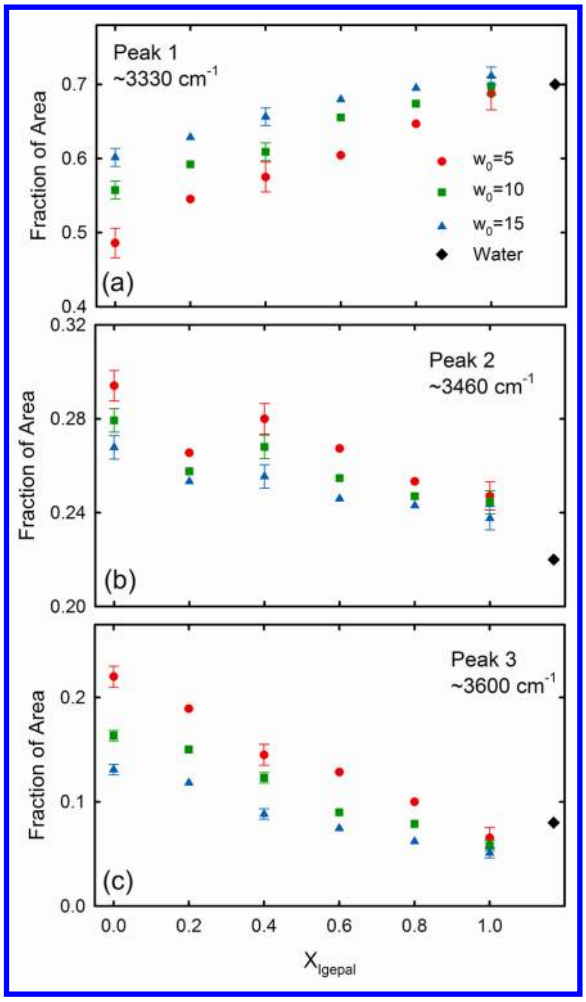

Figure 3. Relative area under curves peaking at 3330 cm^{-1} (a), 3460 cm^{-1} (b), and ∼3600 cm^{-1} (c) for AOT/Igepal/Cy mixed reverse micellar systems at w_0 = 5, 10, and 15.

lower population is compensated by the abundance of "multimer" water in RM. It can also be observed that the relative content of "network" water increases considerably with increasing w_0. On the other hand, Igepal systems show behavior more comparable to that of pure water and an increase in w_0 offers only marginal effect on the relative abundance of "network" water content. It can be argued that the interaction of the water molecules with the hydroxyl headgroup of Igepal[64] is comparable to that of the water−water hydrogen bonded network which eventually results in the elevated population of "network" water. It can also be observed that, with increasing content of Igepal, the relative abundance gradually moves toward that of pure water clearly indicating a linear effect of mixing of surfactants at the interface. The present FTIR measurements strongly corroborate the finding of Brubach et al.[26] who reported that for nonionic fluorocarbon RMs with increasing w_0 and at high surfactant content the fraction of "multimer water" (3600 cm^{-1} region) molecules decreases, which is compensated by increasing "network water" (3330 cm^{-1} region). It is worth mentioning here that such a trend, which is observed in RM systems, is strikingly opposite than that of water confined in "hard" medium. Le Caër et al.[65] recently studied the infrared spectra of water confined in pore glasses as a function of the pore size ranging from 8 to 320 nm in the 30−4000 cm^{-1} spectral range using the attenuated total

dx.doi.org/10.1021/jp3102833 | J. Phys. Chem. B 2013, 117, 3593−3602

Table 1. Emission Maximum (λ_{max}), Biexponential Fitting Parameters of the $C(t)$, and Rotational Anisotropy Decay Curves of C-500 in AOT/Igepal/Cy/Water Mixed RM Systems at Different w_0 and Mixing Ratios

		solvation dynamics			anisotropy		
w_0	λ_{max} (nm)	τ_1 (a_1) (ns)	τ_2 (a_2) (ns)	$\langle\tau_{sol}\rangle$ (ns)	τ_{r1}(a_1) (ns)	τ_{r2} (a_2) (ns)	$\langle\tau_r\rangle$ (ns)
				X_{Igepal} = 0			
5	495	0.12 (0.22)	0.78 (0.78)	0.63	0.46 (0.29)	2.04 (0.71)	1.57
10	497	0.11 (0.23)	0.51 (0.77)	0.42	0.43 (0.37)	1.63 (0.63)	1.18
15	499	0.10 (0.23)	0.48 (0.77)	0.39	0.42 (0.37)	1.24 (0.63)	0.94
				X_{Igepal} = 0.2			
5	494	0.20 (0.48)	1.14 (0.52)	0.69	0.27 (0.46)	1.41 (0.54)	0.88
10	496	0.20 (0.58)	1.05 (0.42)	0.56	0.25 (0.50)	1.20 (0.50)	0.72
15	498	0.21 (0.65)	0.96 (0.35)	0.47	0.23 (0.48)	1.13 (0.52)	0.70
				X_{Igepal} = 0.4			
5	494	0.22 (0.52)	1.35 (0.48)	0.76	0.29 (0.52)	1.35 (0.48)	0.80
10	496	0.22 (0.58)	1.18 (0.42)	0.62	0.24 (0.49)	1.16 (0.51)	0.71
15	498	0.21 (0.64)	1.11 (0.36)	0.53	0.24 (0.50)	1.18 (0.50)	0.71
				X_{Igepal} = 0.6			
5	494	0.22 (0.57)	1.28 (0.43)	0.67	0.27 (0.53)	1.31 (0.47)	0.76
10	496	0.21 (0.58)	1.10 (0.42)	0.58	0.24 (0.50)	1.25 (0.50)	0.74
15	497	0.20 (0.60)	1.08 (0.40)	0.55	0.30 (0.62)	1.57 (0.38)	0.78
				X_{Igepal} = 0.8			
5	493	0.23 (0.57)	1.52 (0.43)	0.78	0.18 (0.55)	1.24 (0.45)	0.66
10	495	0.22 (0.54)	1.31 (0.46)	0.72	0.18 (0.50)	1.13 (0.50)	0.66
15	496	0.21 (0.57)	1.29 (0.43)	0.67	0.23 (0.51)	1.16 (0.49)	0.68
				X_{Igepal} = 1			
5	490	0.20 (0.46)	1.49 (0.54)	0.89	0.21 (0.52)	1.31 (0.48)	0.74
10	492	0.19 (0.49)	1.32 (0.51)	0.77	0.20 (0.55)	1.08 (0.45)	0.60
15	492	0.20 (0.50)	1.24 (0.50)	0.72	0.18 (0.57)	0.95 (0.43)	0.51

reflection (ATR) technique. When the pore size of silica decreases the intensity of the "network" water (~3310 cm^{-1}) component increases and that of the "intermediate" water component (3450 cm^{-1}) decreases, while the contribution of "multimer" water (~3590 cm^{-1}) remains practically unchanged. But in RM, the variations are opposite; i.e., the "intermediate" water contribution decreases with the micelle hydrodynamic radius, whereas the "network" water contribution increases and the "multimer" water component (~3600 cm^{-1}) also decreases. The observed difference may arise due to the more rigid silica walls, as compared to the smoother RM surface. It can be concluded from the IR spectroscopic studies that the synergistic modification of the mechanical properties of the interface does not significantly influence the hydrogen bonded structure of water.

Fluorescence Measurements. A comprehensive understanding of the dynamics of encapsulated water is obtained from steady state and time-resolved fluorescence studies using C-500 as the fluoroprobe. It has been shown that, in RM systems, selective excitation at 409 nm excites the C-500 molecules at the interface only[40] which justifies the choice of the probe. Figure S2 (Supporting Information) depicts the emission spectra of the mixed RM systems at w_0 = 10. The corresponding emission maxima (λ_{max}) are presented in Table 1. C-500 in water produces an emission maximum at ~505 nm, and in AOT/isooctane RM systems it has been reported to suffer a progressive blue shift with decreasing w_0.[40] AOT/Cy RM system at w_0 = 5 produces an emission peak at 495 nm which suffers a red shift of ~4 nm at w_0 = 15 (Table 1). The observed red shift with increasing w_0 is quite intuitive keeping in mind that, once the surfactant headgroup is solvated, the rest of the water molecules only populate the well-structured water pool, thereby increasing the polarity in the vicinity of the surfactant imposing the observed red shift. The emission peak suffers a progressive blue shift with increasing Igepal content along with a broadening of the emission profile. The broadening of the spectral shape could be due to multiple locations of the probe molecules, namely, in "bulk type" water, interfacial water, and deep into the interfacial layer. It should be remembered that C-500 is only sparingly soluble in water and selective excitation of the probe at 409 nm excludes the contribution from the "network" water molecules. We deconvolute the observed spectra of X_{Igepal} = 1 into two Gaussian components with one peak fixed to appear at 500 nm (in accordance with the peak position of the probe residing at the waterpool) and found that the other peak is centered at ~478 nm (Figure S2, Supporting Information). The area under the latter curve is half of that obtained for the former. This relative weighting is found to be invariant of w_0 indicating that the distribution of probe molecules at the Igepal/Cy interface is independent of the water content in the RM.

C-500 has extensively been used as a fluorophore to study the relaxation dynamics of water in confined medium.[40,41,43] In the present study the decay transients of the probe in the blue end of the spectrum could be fitted with multiple decay components, whereas those in the red end could be fitted only by considering an added rise component (Figure S3, Supporting Information). Such an observation is indicative of the solvation of the probe[66] and we construct the solvent correlation function, $C(t)$, following eq 5. Some representative $C(t)$ plots for different X_{Igepal} values at w_0 = 10 are shown in Figure 4a. All the $C(t)$ curves are fitted biexponentially and the time constants are presented in Table 1. As a first step, we check that the observed time-resolved spectral shift is not associated with any internal photophysics of the probe itself. In order to do so we construct the time-resolved area normalized

dx.doi.org/10.1021/jp3102833 | J. Phys. Chem. B 2013, 117, 3593−3602

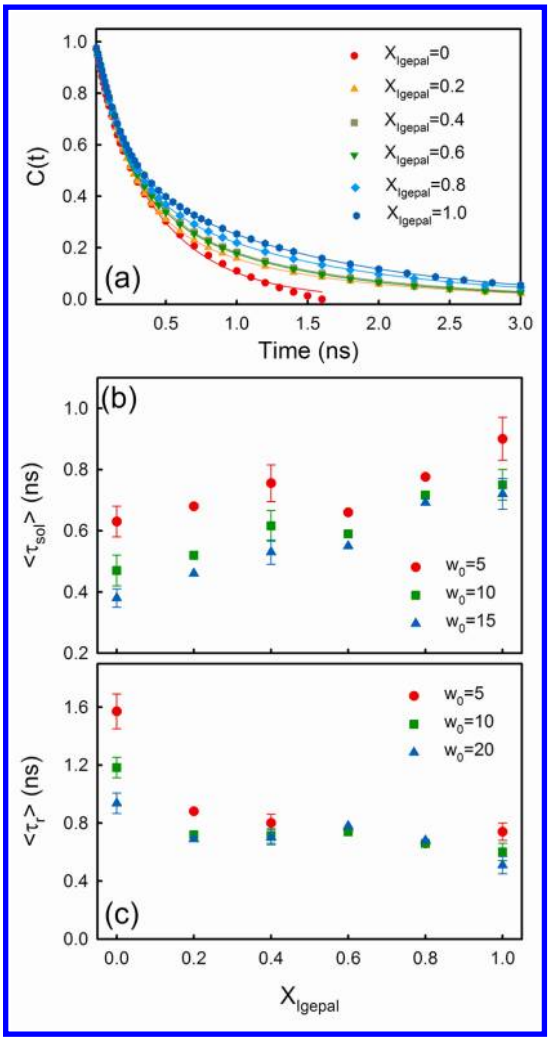

Figure 4. (a) Representative solvent correlation function, $C(t)$ curves of C-500 for AOT/Igepal/Cy reverse micellar systems at w_0 = 10 for different X_{Igepal} values. The solid lines are biexponential fittings. (b) Average solvation time constant $\langle\tau_{sol}\rangle$ as a function of X_{Igepal}. (c) Average rotational time constant $\langle\tau_r\rangle$ as a function of X_{Igepal}.

emission spectra (TRANES)[67] for all these systems. A representative illustration is shown in Figure S3(c). No apparent iso-emissive point is recognized in the TRANES profile, which confirms that the probe contains only a single "species". Therefore, the observed time dependent spectral shift can be attributed solely to the inhomoginity of the micro-environment experienced by the probe. As can be observed from Table 1, the time constants are on the order of hundreds of ps and a few ns, which are orders of magnitude slower than that observed in pure water.[68] It should be taken into consideration that the sub-ps orientational dynamics of water is considerably restricted in the confined systems like RMs. Selective photoexcitation of interfacial probe molecules coupled with the limitation of our instrumental resolution (IRF ~ 80 ps) held us back from detecting the signals responsible for the ultrafast dynamics of water molecules. The reported time scales thus have the sole contribution of water molecules residing at the RM interface only, which is in accord with the essence of this study. We obtain an average Stokes shift of 1000 ± 100 cm^{-1}, which is only ~25% of the Stokes shift calculated from the steady state measurements as intuited from the loss of ultrafast fluorescence signals. We plot the average time constant, $\langle\tau_{solv}\rangle = \sum_i a_i\tau_i$ as a function of X_{Igepal} at three different w_0 values (Figure 4b). It is observed that, with increasing w_0, solvation dynamics gets faster for all these systems. For pure AOT systems the $\langle\tau_{solv}\rangle$ values are in comparable agreement with those obtained in AOT/isooctane RM systems using the same fluorophore.[40] At w_0 = 5, a considerable fraction of water molecules solvate the RM interface and thus exhibit restricted dynamics as evidenced from high $\langle\tau_{solv}\rangle$ values. At $w_0 \geq 10$, a well-defined RM water-pool is built up[45,69,70] and the relative fraction of the slow-moving water molecules gets reduced resulting in an overall faster solvation. It has been observed that $\langle\tau_{solv}\rangle$ is faster in pure AOT systems compared to that in pure Igepal systems. This retardation is attributed to the possible contribution of the terminal hydroxyl groups of Igepal toward the measured relaxation dynamics. $\langle\tau_{solv}\rangle$ does not offer any remarkable pattern around X_{Igepal} = 0.4; instead, an overall increasing trend with X_{Igepal} is registered.

In order to understand the nature of geometrical restriction imposed on the probe molecule by the interfacial layer, we determine the rotational anisotropy of all these systems, and some representative decay transients are shown in Figure S4 (Supporting Information). All the rotational decay transients can be fitted biexponentially and the time constants (τ_r) are presented in Table 1. The observed τ_r values are in comparable agreement with AOT/isooctane systems using the same fluorophore.[40] C-500 in water produces a rotational anisotropy decay time constant of ~70 ps.[71] The observed slow rotational relaxation implies a considerable hindrance inside the RM water pool as experienced by the probe molecules, which reaffirms the solvation dynamics results. It can be observed that the rotation of the probe is eased as w_0 is increased. The restriction is more prominent in the AOT systems, and decreases as Igepal is doped into the interface. The imposed restriction in the AOT system might arise out of the strong interaction of the probe with the surfactant charged interface. As also evidenced from Figure 4c, the change in the average rotational time constant $\langle\tau_r\rangle = \sum_i a_i\tau_{ri}$ follows a fairly linear trend, with a weak dependence on w_0.

General Discussion. In the present contribution we have made a systematic spectroscopic investigation to emphasize any possible correlation between the mechanical properties of a RM interface and physical properties of its adjacent water molecules. Optimization of solubilization capacity of RM is a much anticipated field of research in surface science as high water uptake of RMs is often beneficial for many biophysical applications of RM. It has now been established that increased solubilization capacity involves suitable modification of the mechanical properties of the surfactant monolayer and also of the interaction between the RM droplets.[13] Several previous studies have shown that such an improvement could easily be achieved by blending of surfactants. Mixture of surfactants also brings about desired modification in many applications.[4−9] However, a proper rationale of the process involved is still not vividly understood. In this regard it was pertinent to investigate whether such a modification in the surfactant interface is reflected in the physical properties as well as dynamics of the entrapped water molecules. In our previous study,[36] using mixed surfactant system AOT/Brij-30 in isooctane we concluded that the physical properties and dynamics of water follow a linear trend with mixing. However, in such a system solubilization capacity was limited by the droplet interaction effect as isooctane is a less penetrating hydrocarbon into the

dx.doi.org/10.1021/jp3102833 | J. Phys. Chem. B 2013, 117, 3593−3602

interface. Also, the solubilization behavior did not show any synergistic effect and hence a linear trend in water properties was much intuited. It remains to be answered whether physical properties of water follow a nonlinear trend of interface curvature with mixing.

AOT/Igepal/Cy mixed RM system exhibits synergistic water solubilization behavior with maximum solubilization occurring at a X_{Igepal} = 0.4 mixing ratio (Figure 1). Since the interface of AOT/Cy RM is rigid and noninteracting, the solubilization capacity is primarily governed by the curvature effect. Addition of Igepal induces fluidity in it, which increases its solubilization power. However, in doing so it in turn increases the inter droplet interaction, which eventually limits the extent of solubilization. Thus the interface undergoes a systematic geometric modification with X_{Igepal}. Such a nonlinear behavior allows the system to be a perfect platform to investigate the water structure and dynamics.

DLS studies show a linear increase in droplet size with increasing Igepal doping into the RM interface. Such a linear trend is also noticed in the aggregation number and partial molar volume calculations (Figure 2). O−H stretching vibration as obtained from FTIR measurements in the 3000−3800 cm^{-1} region show three different types of water molecule inside the RMs and progressively follows the linear mixing behavior of the surfactants (Figure 3). FTIR study identifies that the relative population of multimer water component, i.e., water molecules, residing in totally hydrophobic environment is larger in AOT RM compared to that in Igepal RM, and it follows an overall linear trend with X_{Igepal} and eventually resembles the values of pure water. No marked deviation from the linear trend is observed in the maximum solubilization region. Sub-ns relaxation dynamics of the entrapped water as revealed by the time-resolved fluorescence spectroscopy using C-500 as the probe identifies the confined nature of the entrapped water in all the studied systems, a behavior markedly different from that in pure water. The dynamics, however, shows a gradual change with the change in interface stoichiometry and any characteristic feature around the solubilization inflation point is not unambiguously noticed. It therefore emerges that changes in the mechanical properties of surfactant film merely affect the structure and relaxation dynamics of the entrapped water molecules, which is believed to essentially be governed by the water content and the surface charge type only.

CONCLUSIONS

In AOT/Igepal/Cy mixed surfactant systems a 5-fold increase in solubilization capacity is obtained compared to that of the constituent surfactants at X_{Igepal} = 0.4. DLS studies show a linear increase in the droplet size with X_{Igepal}. Densimetric and acoustic measurements also do not reveal any characteristic feature around the maximum solubilization point. FTIR study in the 3000−3800 cm^{-1} region identifies that the relative population of "multimer" water component, i.e., water molecules residing mostly in hydrophobic environment is larger in AOT RM compared to that in Igepal RM, and it follows a linear trend with X_{Igepal}. Sub-ns relaxation dynamics of the entrapped water as revealed by C-500 also exhibits a more or less linear trend with no characteristic feature around the solubilization inflation point. These results conclude that the changes in the mechanical properties of RM interface barely affect the slow relaxation dynamics of the entrapped water molecules.

ASSOCIATED CONTENT

Supporting Information

Calculation of aggregation number, DLS, volumetric, and densimetric measurement parameters, FTIR spectra, and emission spectra. This material is available free of charge via the Internet at http://pubs.acs.org.

AUTHOR INFORMATION

Corresponding Author

*Phone: 91-33-23355706. Fax: 91-33-23353477. E-mail: rajib@bose.res.in.

Notes

The authors declare no competing financial interest.

ACKNOWLEDGMENTS

A.D. acknowledges UGC, Government of India, for a research fellowship. R.K.M. acknowledges CSIR for a research grant (no. 01(2573)/12/EMR-II) and Theme Unit of Excellence on Nanodevice Technology at SNBNCBS for support.

REFERENCES

(1) Moulik, S. P.; Paul, B. K. Structure, Dynamics and Transport Properties of Microemulsions. *Adv. Colloid Interface Sci.* **1998**, *78*, 99−195.

(2) Johnson, K. A.; Shah, D. O. Effect of Oil Chain Length and Electrolytes on Water Solubilization in Alcohol-free Pharmaceutical Microemulsions. *J. Colloid Interface Sci.* **1985**, *107*, 269−271.

(3) Lundsten, G.; Backlund, S.; Kiwilsza, G. Solubility Limits of Water in Systems of Aromatic Oils and Non-ionic Surfactants. *Prog. Colloid Polym. Sci.* **1994**, *97*, 194−198.

(4) Shome, A.; Roy, S.; Das, P. Nonionic Surfactants: A Key to Enhance the Enzyme Activity at Cationic Reverse Micellar Interface. *Langmuir* **2007**, *23*, 4130−4136.

(5) Chen, D.-H.; Liao, M.-H. Effects of Mixed Reverse Micellar Structure on Stability and Activity of Yeast Alcohol Dehydrogenase. *J. Mol. Cat. B: Enzym.* **2002**, *18*, 155−162.

(6) Lan, J.; Zhang, Y.; Huang, X.; Hu, M.; Liu, W.; Li, Y.; Qu, Y.; Gao, P. Improvement of the Catalytic Performance of Lignin Peroxidase in Reversed Micelles. *J. Chem. Tech. Biotech.* **2008**, *83*, 64−70.

(7) Poulsen, A. K.; Arleth, L.; Almdal, K.; Scharff-Poulsen, A. M. Unusually Large Acrylamide Induced Effect on the Droplet Size in AOT/Brij30 Water-in-oil Microemulsions. *J. Colloid Interface Sci.* **2007**, *306*, 143−153.

(8) Zhang, J.; Han, B.; Liu, J.; Zhang, X.; He, J.; Liu, Z.; Jiang, T.; Yang, G. Recovery of Silver Nanoparticles Synthesized in AOT/C12E4Mixed Reverse Micelles by Antisolvent CO2. *Chem.—Eur. J.* **2002**, *8*, 3879−3883.

(9) Singh, P. K.; Satpati, A. K.; Kumbhakar, M.; Pal, H.; Nath, S. A Nanoreactor for Tuning the Chemical Reactivity of a Solute. *J. Phys Chem. B* **2008**, *112*, 11447−11450.

(10) Melo, E. P.; Aires-Barros, M. R.; Cabral, J. M. S. Reverse Micelles and Protein Biotechnology Original Research Article. *Biotechnol. Ann. Rev.* **2001**, *7*, 87−129.

(11) Streitner, N.; Voss, C.; Flaschel, E. Reverse Micellar Extraction Systems for the Purification of Pharmaceutical Grade Plasmid DNA. *J. Biotechnol.* **2007**, *131*, 188−196.

(12) Furusaki, S.; Ichikawa, S.; Goto, M. Recent Advances in Reversed Micellar Techniques for Bioseparation. *Prog. Biotechnol.* **2000**, *16*, 133−136.

(13) Hou, M. J.; Shah, D. O. Effects of the Molecular Structure of the Interface and Continuous Phase on Solubilization of Water in Water/Oil Microemulsions. *Langmuir* **1987**, *3*, 1086−1096.

(14) Huibers, P. D. T.; Shah, D. O. Evidence for Synergism in Nonionic Surfactant Mixtures: Enhancement of Solubilization in Water-in-Oil Microemulsions. *Langmuir* **1997**, *13*, 5762−5765.

(15) Mitra, R. K.; Paul, B. K. Effect of NaCl and Temperature on the Water Solubilization Behavior of AOT/Nonionics Mixed Reverse Micellar Systems Stabilized in IPM Oil. *Colloids Surf., A* **2005**, *255*, 165−180.
(16) Paul, B. K.; Mitra, R. K. Water Solubilization Capacity of Mixed Reverse Micelles: Effect of Surfactant Component, the Nature of the Oil, and Electrolyte Concentration. *J. Colloid Interface Sci.* **2005**, *288*, 261−279.
(17) Mitra, R. K.; Paul, B. K. Investigation on Percolation in Conductance of Mixed Reverse Micelles. *Colloids Surf., A* **2005**, *252*, 243−259.
(18) Mitra, R. K.; Paul, B. K.; Moulik, S. P. Phase Behavior, Interfacial Composition and Thermodynamic Properties of Mixed Surfactant (CTAB and Brij-58) Derived w/o Microemulsions with 1-butanol and 1-pentanol as Cosurfactants and n-heptane and n-decane as Oils. *J. Colloid Interface Sci.* **2006**, *300*, 755−764.
(19) Kinugasa, T.; Kondo, A.; Nishimura, S.; Miyauchi, Y.; Nishii, Y.; Watanabe, K.; Takeuchi, H. Estimation for Size of Reverse Micelles Formed by AOT and SDEHP Based on Viscosity Measurement. *Colloids Surf., A* **2002**, *204*, 193−199.
(20) Liu, D.; Ma, J.; Cheng, H.; Zhao, Z. Fluorescence Probing of Mixed Reverse Micelles Formed with AOT and Nonionic Surfactants in n-heptane. *Colloids Surf., A* **1998**, *139*, 21−26.
(21) Chatterjee, S.; Mitra, R. K.; Paul, B. K.; Bhattacharya, S. C. Interface of AOT/Brij Mixed Reverse Micellar Systems: Conductometric and Spectrophotometric Investigations. *J. Colloid Interface Sci.* **2006**, *298*, 935−941.
(22) Chatterjee, S.; Nandi, S.; Bhattacharya, S. C. Interface of AOT/Igepal CO720/Cyclohexane/Water Mixed Reverse Micelle by Spectroscopic Approach. *Colloids Surf., A* **2006**, *279*, 58−63.
(23) Bumajdad, A.; Eastoe, J.; Heenan, R. K.; Lu, R. J.; Steytler, D. C. S.; Egelhaaf, S., E. Mixing in Cationic Surfactant Films Studied by Small-angle Neutron Scattering. *J. Chem. Soc., Faraday Trans.* **1998**, *94*, 2143−2150.
(24) Bumajdad, A.; Eastoe, J.; Griffiths, P.; Steytler, D. C.; Heenan, R. K.; Lu, J. R.; Timmins, P. Interfacial Compositions and Phase Structures in Mixed Surfactant Microemulsions. *Langmuir* **1999**, *15*, 5271−5278.
(25) Bumajdad, A.; Eastoe, J.; Nave, S.; Steytler, D. C.; Heenan, R. K.; Grillo, I. Compositions of Mixed Surfactant Layers in Microemulsions Determined by Small-Angle Neutron Scattering. *Langmuir* **2003**, *19*, 2560−2567.
(26) Brubach, J.-B.; Mermet, A.; Filabozzi, A.; Gerschel, A.; Lairez, D.; Krafft, M. P.; Roy, P. Dependence of Water Dynamics upon Confinement Size. *J. Phys. Chem. B* **2001**, *105*, 430−435.
(27) Li, Q.; Li, T.; Wu, J. Comparative Study on the Structure of Reverse Micelles. 2. FT-IR, 1H NMR, and Electrical Conductance of H2O/AOT/NaDEHP/n-Heptane Systems. *J. Phys. Chem. B* **2000**, *104*, 9011−9016.
(28) Bhattacharyya, K. Solvation Dynamics and Proton Transfer in Supramolecular Assemblies. *Acc. Chem. Res.* **2003**, *36*, 95−101.
(29) Fayer, M. D. Water in a Crowd. *Physiology* **2011**, *26*, 381−392.
(30) Moilanen, D. E.; Levinger, N. E.; Spry, D. B.; Fayer, M. D. Confinement or the Nature of the Interface? Dynamics of Nanoscopic Water. *J. Am. Chem. Soc.* **2007**, *129*, 14311−14318.
(31) Pant, D.; Levinger, N. E. Polar Solvation Dynamics in Nonionic Reverse Micelles and Model Polymer Solutions. *Langmuir* **2000**, *16*, 10123−10130.
(32) Pant, D.; Riter, R. E.; Levinger, N. E. Influence of Restricted Environment and Ionic Interactions on Water Solvation Dynamics. *J. Chem. Phys.* **1998**, *109*, 9995−10003.
(33) Riter, R. E.; Undiks, E. P.; Levinger, N. E. Impact of Counterion on Water Motion in Aerosol OT Reverse Micelles. *J. Am. Chem. Soc.* **1998**, *120*, 6062−6067.
(34) Narayanan, S. S.; Sinha, S. S.; Sarkar, R.; Pal, S. K. Validation and Divergence of the Activation Energy Barrier Crossing Transition at AOT/Lecithin Reverse Micellar Interface. *J. Phys. Chem. B* **2008**, *112*, 2859−2867.
(35) Narayanan, S. S.; Sinha, S. S.; Sarkar, R.; Pal, S. K. Picosecond to Nanosecond Reorganization of Water in AOT/Lecithin Mixed Reverse Micelles of Different Morphology. *Chem. Phys. Lett.* **2008**, *452*, 99−104.
(36) Mitra, R. K.; Sinha, S. S.; Verma, P. K.; Pal, S. K. Modulation of Dynamics and Reactivity of Water in Reverse Micelles of Mixed Surfactants. *J. Phys. Chem. B* **2008**, *112* (41), 12946−12953.
(37) Nave, S.; Eastoe, J.; Heenan, R. K.; Steytler, D.; Grillo, I. What Is So Special about Aerosol-OT? 2. Microemulsion Systems. *Langmuir* **2000**, *16*, 8741−8748.
(38) Lipgens, S.; Schuebel, D.; Schlicht, L.; Spilgies, J.-H.; Ilgenfritz, G.; Eastoe, J.; Heenan, R. K. Percolation in Nonionic Water (w/o)-Microemulsion Systems: A Small Angle Neutron Scattering Study. *Langmuir* **1998**, *14*, 1041−1049.
(39) Mitra, R. K.; Sinha, S. S.; Pal, S. K. Temperature Dependent Hydration at Micellar Surface: Activation Energy Barrier Crossing Model Revisited. *J. Phys. Chem. B* **2007**, *111*, 7577−7581.
(40) Mitra, R. K.; Sinha, S. S.; Pal, S. K. Temperature-Dependent Solvation Dynamics of Water in Sodium Bis(2-ethylhexyl)-sulfosuccinate/Isooctane Reverse Micelles. *Langmuir* **2008**, *24*, 49−56.
(41) Patra, A.; Verma, P. K.; Mitra, R. K. Slow Relaxation Dynamics of Water in Hydroxypropyl Cellulose-Water Mixture Traces Its Phase Transition Pathway: A Spectroscopic Investigation. *J. Phys. Chem. B* **2012**, *116*, 1508−1516.
(42) Verma, P. K.; Makhal, A.; Mitra, R. K.; Pal, S. K. Role of Solvation Dynamics in the Kinetics of Solvolysis Reactions in Microreactors. *Phys. Chem. Chem. Phys.* **2009**, *11*, 8467−8476.
(43) Verma, P. K.; Saha, R.; Mitra, R. K.; Pal, S. K. Slow Water Dynamics at the Surface of Macromolecular Assemblies of Different Morphologies. *Soft Matter* **2010**, *6*, 5971−5979.
(44) Verma, P. K.; Mitra, R. K.; Pal, S. K. A Molecular Picture of Diffusion Controlled Reaction: Role of Microviscosity and Hydration on Hydrolysis of Benzoyl Chloride at a Polymer Hydration Region. *Langmuir* **2009**, *25*, 11336−11343.
(45) Amararene, A.; Gindre, M.; Le Huérou, J.-Y.; Urbach, W.; Valdez, D.; Waks, M. Adiabatic compressibility of AOT [sodium bis(2-ethylhexyl)sulfosuccinate] Reverse micelles: Analysis of a Simple Model Based on Micellar Size and Volumetric Measurements. *Phys. Rev. E* **2000**, *61*, 682−689.
(46) Zamyatnin, A. A. Amino Acid, Peptide, and Protein Volume in Solution. *Annu. Rev. Biophys. Bioeng.* **1984**, *13*, 145−165.
(47) Sarvazyan, A. P. Ultrasonic Velocimetry of Biological Compounds. *Annu. Rev. Biophys. Biophys. Chem.* **1991**, *20*, 321−342.
(48) O'Connor, D. V.; Philips, D., *Time Correlated Single Photon Counting*; Academic Press: London, 1984.
(49) Seedher, N.; Manik, M. Solubilization in Mixed Surfactant Reverse Micellar Systems. *J. Surface Sci. Technol.* **1993**, *9*, 81−86.
(50) Ruckenstein, E.; Chi, J. C. Stability of Microemulsions. *J. Chem. Soc., Faraday Trans. 2* **1975**, *71*, 1690−1707.
(51) Ruckenstein, E.; Krishnan, R. Swollen Micellar Models for Solubilization. *J. Colloid Interface Sci.* **1979**, *71*, 321−335.
(52) Moulik, S. P.; De, G. C.; Bhowmik, B. B.; Panda, A. K. Physicochemical Studies on Microemulsions. 6. Phase Behavior, Dynamics of Percolation, and Energetics of Droplet Clustering in Water/AOT/n-Heptane System Influenced by Additives (Sodium Cholate and Sodium Salicylate). *J. Phys. Chem. B* **1999**, *103*, 7122−7129.
(53) Maitra, A. Determination of Size Parameters of Water-Aerosol OT-Oil Reverse Micelles from Their Nuclear Magnetic Resonance Data. *J. Phys. Chem.* **1984**, *88*, 5122−5125.
(54) Banerjee, D.; Sinha, S. S.; Pal, S. K. Interplay between Hydration and Electrostatic Attraction in Ligand Binding: Direct Observation of Hydration Barrier at Reverse Micellar Interface. *J. Phys. Chem. B* **2007**, *111*, 14239−14243.
(55) Amararene, A.; Gindre, M.; Le Huerou, J.-Y.; Nicot, C.; Urbach, W.; Waks, M. Water Confined in Reverse Micelles: Acoustic and Densimetric Studies. *J. Phys. Chem. B* **1997**, *101*, 10751−10756.

(56) Lock, A. J.; Bakker, H. J. Temperature Dependence of Vibrational Relaxation in Liquid H2O. *J. Chem. Phys.* **2002**, *117*, 1708−1713.
(57) Corcelli, S. A.; Skinner, J. L. Infrared and Raman Line Shapes of Dilute HOD in Liquid H2O and D2O from 10 to 90 °C. *J. Phys. Chem. A* **2005**, *109*, 6154−6165.
(58) Graener, H.; Seifert, G. Vibrational and Orientational Relaxation of Monomeric Water Molecules in Liquids. *J. Chem. Phys.* **1993**, *98*, 36−45.
(59) Scatena, L. F.; Brown, M. G.; Richmond, G. L. Water at Hydrophobic Surfaces: Weak Hydrogen Bonding and Strong Orientation Effects. *Science* **2001**, *292*, 908−912.
(60) Zhou, N.; Li, Q.; Wu, J.; Chen, J.; Weng, S.; Xu, G. Spectroscopic Characterization of Solubilized Water in Reversed Micelles and Microemulsions: Sodium Bis(2-ethylhexyl) Sulfosuccinate and Sodium Bis(2-ethylhexyl) Phosphate in n-Heptane. *Langmuir* **2001**, *17*, 4505−4509.
(61) Zhong, Q.; Steinhurst, D. A.; Carpenter, E. E.; Owrutsky, J. C. Fourier Transform Infrared Spectroscopy of Azide Ion in Reverse Micelles. *Langmuir* **2002**, *18*, 7401−7408.
(62) Bhattacharyya, K.; Bagchi, B. Slow Dynamics of Constrained Water in Complex Geometries. *J. Phys. Chem. A* **2000**, *104* (46), 10603−10613.
(63) Pal, S. K.; Peon, J.; Bagchi, B.; Zewail, A. H. Biological Water: Femtosecond Dynamics of Macromolecular Hydration. *J. Phys. Chem. B* **2002**, *106*, 12376−12395.
(64) Fenn, E. E.; Wong, D. B.; Fayer, M. D. Water Dynamics at Neutral and Ionic Interfaces. *Proc. Natl. Acad. Sci. U.S.A.* **2009**, *106*, 15243−15248.
(65) Caër, S. L.; Pin, S.; Esnouf, S.; Raffy, Q.; Renault, J. P.; Brubach, J.-B.; Creff, G.; Roy, P.; Trapped Water, A. Network in Nanoporous Material: The Role of Interfaces. *Phys. Chem. Chem. Phys.* **2011**, *13*, 17658−17666.
(66) Maroncelli, M.; Fleming, G. R. Picosecond Solvation Dynamics of Coumarin 153: The Importance of Molecular Aspects of Solvation. *J. Chem. Phys.* **1987**, *86*, 6221−6238.
(67) Koti, A. S. R.; Krishna, M. M. G.; Periasamy, N. Time-Resolved Area-Normalized Emission Spectroscopy (TRANES): A Novel Method for Confirming Emission from Two Excited States. *J. Phys. Chem. A* **2001**, *105*, 1767−1771.
(68) Jimenez, R.; Fleming, G. R.; Kumar, P. V.; Maroncelli, M. Femtosecond Solvation Dynamics of Water. *Nature* **1994**, *369*, 471−473.
(69) D'Angelo, M.; Fioretto, D.; Onori, G.; Palmieri, L.; Santucci, A. Dynamics of Water-Containing Sodium Bis(2-ethylhexyl)-sulfosuccinate (AOT) Reverse Micelles: A High-Frequency Dielectric Study. *Phys. Rev. E* **1996**, *54*, 993−996.
(70) Carlstroem, G.; Halle, B. Water Dynamics in Microemulsion Droplets. A Nuclear Spin Relaxation Study. *Langmuir* **1988**, *4*, 1346−1352.
(71) Banerjee, D.; Verma, P. K.; Pal, S. K. A Temperature Dependent Femtosecond-Resolved Hydration Dynamics of Water in Aqueous Guanidinium Hydrochloride Solution. *Photochem. Photobiol. Sci.* **2009**, *8*, 1441−1447.